

A Coupled Magnetic-Elastic-Thermal Free-Energy Model with Hysteretic Nonlinearity for Terfenol-D Rods

Tian-Zhong Wang¹ and You-He Zhou^{1,2}

Abstract: Based on the thermodynamic theory and the postulates of Jiles and Atherton, a general coupled magnetic-elastic-thermal free-energy model with hysteretic nonlinearity is established for Terfenol-D rods, in which the effect of Weiss molecular field is incorporated. The quantitative agreement between numerical simulation results predicted by the free-energy model and existing experimental data confirms the validity and reliability of the obtained nonlinear theoretical model, and indicates that the free-energy model can accurately capture the nonlinear hysteresis characteristic of Terfenol-D. Meanwhile, the free-energy model is employed to investigate the influences of mechanical stress and the temperature on the magnetostrictive effect of Terfenol-D in detail, and its predictions are coincident with some well-known experimental results including the temperature-dependent saturation nonlinearity and “overturn phenomenon”. It indicates that the free-energy model can also effectively capture the nonlinear magnetic-elastic-thermal coupling characteristic of Terfenol-D. Some important physical parameters, such as the maximum magnetostrictive strain, the maximum piezomagnetic coefficient, are summarized, which can be used to optimize the performance of Terfenol-D in practical application. In addition, the free-energy model uses simple differential equation and algebraic equations, in which all of parameters have definite physical implications and can be easily determined by experiments. Thus, the free-energy model established in this article has very strong and wide practicability.

Keywords: Terfenol-D, hysteresis, magnetic-elastic-thermal coupling, nonlinearity.

¹ Key Laboratory of Mechanics on Disaster and Environment in Western China, Ministry of Education of China, and Department of Mechanics, Lanzhou University, Lanzhou 730000, People's Republic of China.

² Corresponding author: Tel:86-0931-8910340; Fax:86-0931-8625576; E-mail: zhouyh@lzu.edu.cn

1 Introduction

Terfenol-D ($\text{Tb}_{0.3}\text{Dy}_{0.7}\text{Fe}_{1.93}$), which is widely used in micro-sensors, robotics, ultrasonic transducers, resonators, active vibration absorbers, linear motors, micro-pumps, micro-valves, micro-positioners, etc, has stimulated an increasing number of research activities due to its distinct characteristics such as high magnetostrictive strain, fast response, simple driving, high energy coupling factor, wide frequency rang, good low frequency character and so on [Olabi and Grunwald (2008); Zhou, Li, Ye, Zhao, Xia, Tang, and Wei (2010)]. Like any other smart material, however, many experiments have shown that the magnetostrictive effect of magnetostrictive materials (e.g., Terfenol-D) exhibits nonlinear hysteresis and magnetic-elastic-thermal coupling constitutive behavior [Clark, Teter, and McMasters (1988); Gao, Pei, and Fang (2008); Liang and Zheng (2007); Moffett, Clark, Wun-Fogle, Linberg, Teter, and McLaughlin (1991)], which make it difficult to accurately model the magnetostrictive effect and hinder their wider applicability in practice. That is, both magnetization-applied field curve and magnetostrictive strain-applied field curve are nonlinear, highly sensitive to the mechanical stress and environmental temperature, and irreversible duo to hysteresis. This is due to inherent magnetic properties of the materials and is particularly pronounced at higher drive levels. Therefore, from both the fundamental perspective of material characterization and future material development, and the practical perspective of transducer design and model-based control development, it is quite significant and necessary to establish a general theoretical model simultaneously incorporating nonlinear hysteresis and magnetic-elastic-thermal coupling constitutive behavior inherent to Terfenol-D.

Initial models quantifying the magnetostrictive effect of Terfenol-D are based on the linear constitutive piezomagnetic equations [Clark (1980)], which, however, are single value relationships and accurate only within a small operating rang. In order to effectively reflect nonlinear characteristics of magnetostrictive effect, some nonlinear constitutive models have been developed including the standard square model [Carman and Mitrovic (1995)], the hyperbolic tangent model [Wan, Fang, and Hwang (2003)], the model based on density of domain switching [Wan, Fang, and Hwang (2003)] and the Zheng-Liu model [Zheng and Liu (2005)] as well as the model derived by Duenas *et al* [Duenas, Hsu, and Carman (1996)]. Among these nonlinear constitutive models, it should be emphasized that the Zheng-Liu model can quantitatively predict all nonlinear magnetic-elastic coupling characteristics and has wider applicability and higher precision than any other nonlinear model listed above, which has been successfully used in the magnetoelectric composites and the beams laminated with giant magnetostrictive actuators [Wang and Zhou (2010); Zhou, Zhou, and Zheng (2007)]. However, the Zheng-Liu model can not describe temperature effect and hysteretic nonlinearity inherent to materials.

Hysteresis models for Terfenol-D can be roughly classified into physics-based models and phenomenological models. The most popular phenomenological hysteresis model used to characterize hysteretic phenomenon of Terfenol-D is the Preisach model [Bergqvist and Engdahl (1991)]. Whereas this model can efficiently describe the nonlinear magnetic-elastic effect of Terfenol-D, it lacks physical meaning and requires a large number of nonphysical parameters to be identified, and thus is not easily adapted to changing operating conditions. Physics-based models are built on first principles of physics, examples of which are the Jiles-Atherton model [Jiles and Atherton (1983)] for ferromagnetic hysteresis and its extended models [Calkins, Smith, and Flatau (2000)]. The characteristics of these models, including the use of few physically related material parameters and computational efficiency, make them applicable to a broader performance space. However, all of these physics-based models do not sufficiently consider the nonlinear magnetic-elastic-thermal coupling constitutive behavior exhibited by Terfenol-D, especially for the effect of temperature. Since the intelligent devices designed with Terfenol-D are unavoidably operated in an environment of varied temperature in practice, the influence of temperature on the magnetostrictive effect can not be neglected. Although Smith et al. [Smith, Seelecke, Dapino, and Ounaies (2006)] investigate thermally activated relaxation characteristics for ferromagnetic materials, they focus solely on the effect of heat on the relaxation behavior of the materials, and the effect of temperature on the magnetic-elastic-thermal coupling constitutive behavior itself of Terfenol-D is not taken into account in their theory. Thus, a general physics-based theoretical model with the capability for simultaneously and conveniently describing the nonlinear hysteresis and magnetic-elastic-thermal coupling constitutive behavior of Terfenol-D is still lacking.

In this article, we focus on the nonlinear characteristics of hysteresis and magnetic-elastic-thermal coupling constitutive behavior inherent to Terfenol-D. Based on the thermodynamic theory and the postulates of Jiles and Atherton, a general coupled magnetic-elastic-thermal free-energy model with hysteretic nonlinearity is developed in Sec. 2. The validity and reliability of the obtained theoretical model are verified in Sec. 3 by comparing its predicted results with those existing experimental data, wherein the effect of Weiss molecular field, and the influences of the mechanical stress and the temperature on the magnetostrictive effect of Terfenol-D are also discussed. The conclusions are summarized in Sec. 4.

2 Theoretical framework

In this section, we briefly display the derivation process of the coupled magnetic-elastic-thermal free-energy model with hysteretic nonlinearity for Terfenol-D. Considering Terfenol-D is often prepared in the form of rod, which is usually subjected

to an axial external stress and an axial applied magnetic field as well as working temperature for practical application, here, a one-dimension model is mainly investigated for Terfenol-D rods. However, the method used in this article can also be generalized to the corresponding three-dimension model, which has been successfully implemented in the single value constitutive model used to describe magnetic-elastic coupling constitutive behavior for giant magnetostrictive materials and deformable magnetized medium without consideration of temperature effect [Liu and Zheng (2005); Zhou, Zhou, Zheng, and Wei (2009)]. The one-dimension free-energy model for Terfenol-D rods consists of a magnetostriction model with a magnetization model.

2.1 Magnetostriction model

As a kind of magnetostrictive material, a Terfenol-D rod is generally supposed to be a thermodynamics system. For this thermodynamics system, the total differential of the internal energy density function U can be expressed as follows [Wang (1992)]:

$$dU = TdS + \sigma d\varepsilon - \mu_0 M dH \quad (1)$$

Here, T is the temperature, S is the entropy density, σ is the stress, ε is the strain, $\mu_0 = 4\pi \times 10^{-7} \text{H/m}$ is the vacuum permeability, H and M are the applied magnetic field and the corresponding magnetization, respectively. Then, the corresponding Gibbs free energy density function G for this thermodynamics system can be written as

$$G = U - TS - \sigma\varepsilon + \mu_0 MH \quad (2)$$

Thus, its total differential is

$$dG = dU - TdS - SdT - \sigma d\varepsilon - \varepsilon d\sigma + \mu_0 M dH + \mu_0 H dM \quad (3)$$

Substituting Eq. (1) into Eq. (3), then gives

$$dG = -\varepsilon d\sigma - SdT + \mu_0 H dM \quad (4)$$

Thereby, in term of a Legendre transform, the strain is given by

$$\varepsilon = -\frac{\partial G}{\partial \sigma} \quad (5)$$

Choosing the stress σ , the temperature T and the magnetization M as independent variables, the Gibbs free energy density function $G(\sigma, M, T)$ can be rewritten by a

Taylor series expansion around the reference point $(\sigma, M, T) = (0, 0, T_r)$, where T_r is the spin reorientation temperature and $T_r = 0$ °C for Terfenol-D [AI-Jiboory and Lord (1990)], i.e.,

$$G(\sigma, M, T) = G(0, 0, T_r) + \sum_{n=1}^{\infty} \frac{1}{n!} \left[\frac{\partial}{\partial \sigma} \sigma + \frac{\partial}{\partial M} M + \frac{\partial}{\partial T} (T - T_r) \right]^n G(\sigma, M, T) \quad (6)$$

where $G(0, 0, T_r)$ is supposed to be zero. Then, by substituting Eq. (6) into Eq. (5), the polynomial strain expansions can be obtained based on the truncated polynomial energy density expansion:

$$\begin{aligned} \varepsilon(\sigma, M, T) = & -\frac{\partial^2 G}{\partial \sigma^2} \sigma - \frac{1}{2} \frac{\partial^3 G}{\partial \sigma^3} \sigma^2 - \frac{1}{3!} \frac{\partial^4 G}{\partial \sigma^4} \sigma^3 - \dots \\ & - \frac{1}{2} \left(\frac{\partial^3 G}{\partial \sigma \partial M^2} + \frac{\partial^4 G}{\partial \sigma^2 \partial M^2} \sigma + \dots \right) M^2 \\ & - \frac{\partial^2 G}{\partial T \partial \sigma} (T - T_r) - \frac{1}{2} \frac{\partial^4 G}{\partial T \partial \sigma \partial M^2} (T - T_r) M^2 \end{aligned} \quad (7)$$

Here, the symmetric properties on the magnetization M are taken into account in the above expansions [Clark (1980)]. It should be noted that the partial derivatives before the independent variables are all calculated at the reference point $(0, 0, T_r)$. Thus, all the partial derivatives in the above strain expansions are coefficients or constants. In order to rationally characterize these coefficients, we firstly rewrite Eq. (7) in a compact form

$$\varepsilon(\sigma, M, T) = \frac{\sigma}{E_s} + \lambda_0(\sigma) + \frac{\lambda_{\max}(\sigma)}{M_s^2} M^2 + \alpha (T - T_r) - \frac{\tilde{B}}{M_s^2} (T - T_r) M^2 \quad (8)$$

Here,

$$\frac{\sigma}{E_s} + \lambda_0(\sigma) = -\frac{\partial^2 G}{\partial \sigma^2} \sigma - \frac{1}{2} \frac{\partial^3 G}{\partial \sigma^3} \sigma^2 - \frac{1}{3!} \frac{\partial^4 G}{\partial \sigma^4} \sigma^3 - \dots \quad (9)$$

$$\frac{\lambda_{\max}(\sigma)}{M_s^2} = -\frac{1}{2} \left(\frac{\partial^3 G}{\partial \sigma \partial M^2} + \frac{\partial^4 G}{\partial \sigma^2 \partial M^2} \sigma + \dots \right) \quad (10)$$

$$\alpha = -\frac{\partial^2 G}{\partial T \partial \sigma} \quad (11)$$

$$\frac{\tilde{B}}{M_s^2} = \frac{1}{2} \frac{\partial^4 G}{\partial T \partial \sigma \partial M^2} \quad (12)$$

in which M_s represents the saturation magnetization when $T = T_r$, E_s is the intrinsic Young's modulus at the saturation segment, α is the constant of thermal expansion, and \tilde{B} is the slope determined by the saturation magnetostrictive strain-temperature curve, which is a constant independent on the temperature due to the linear dependence of the saturation magnetostrictive strain on the temperature for Terfenol-D [Clark and Crowder (1985)].

Some well-known experiments have indicated the main characteristics of stress-strain curve for Terfenol-D rods [Butler (1988); Kellogg and Flatau (1999)]. Based on these main characteristics, the nonlinear strain $\lambda_0(\sigma)$ and the maximum strain $\lambda_{\max}(\sigma)$ can be respectively chosen as

$$\bar{\lambda}_0(\bar{\sigma}) = \begin{cases} \tanh(\bar{\sigma}) & (\bar{\sigma} \geq 0) \\ \tanh(2\bar{\sigma})/2 & (\bar{\sigma} < 0) \end{cases} \quad (13)$$

$$\lambda_{\max}(\sigma) = \lambda_s - \lambda_0(\sigma) \quad (14)$$

in which $\bar{\lambda}_0(\bar{\sigma}) = \frac{\lambda_0(\sigma)}{\lambda_s}$ and $\bar{\sigma} = \frac{\sigma}{\sigma_s}$ are, respectively, the dimensionless quantities of $\lambda_0(\sigma)$ and σ , λ_s is the saturation magnetostrictive coefficient, and $\sigma_s = \frac{\lambda_s E_s E_0}{(E_s - E_0)}$ is the reference stress, in which E_0 is the initial Young's modulus. The detailed discussion about these two nonlinear functions can be found in the case of magnetic-elastic coupling constitutive behavior for giant magnetostrictive materials without consideration of temperature effect [Zheng and Liu (2005)].

Direct substitution of Eqs. (13) and (14) into Eq. (8) yields the following analytical formula of the magnetostriction model,

$$\varepsilon(\sigma, M, T) = \frac{\sigma}{E_s} + \alpha(T - T_r) - \frac{\tilde{B}}{M_s^2}(T - T_r)M^2 + \begin{cases} \lambda_s \tanh\left(\frac{\sigma}{\sigma_s}\right) + \frac{[1 - \tanh(\frac{\sigma}{\sigma_s})]\lambda_s}{M_s^2} M^2 & (\frac{\sigma}{\sigma_s} \geq 0) \\ \frac{\lambda_s}{2} \tanh\left(\frac{2\sigma}{\sigma_s}\right) + \frac{[2 - \tanh(\frac{2\sigma}{\sigma_s})]\lambda_s}{2M_s^2} M^2 & (\frac{\sigma}{\sigma_s} < 0) \end{cases} \quad (15)$$

According to Eq. (15), it is obvious that the magnetostriction model is nonlinear and consists of four kinds of terms, i.e., elastic strain term, magnetic-elastic coupling term and thermal expansion term as well as magnetic-thermal coupling term. That is, the nonlinear magnetic-elastic-thermal coupling constitutive behavior inherent to Terfenol-D is sufficiently reflected in the magnetostriction model, especially for the effect of temperature. Thus, the model is suitable for magnetostrictive materials under various mechanical and magnetic loading conditions as well as working temperature. Meanwhile, this model only involves six material constants, i.e., E_s , α , \tilde{B} , M_s , λ_s and σ_s , which have definite physical implications

and can be easily determined by experiments. Therefore, the model can be directly and conveniently used in engineering application. Here, the strain which is induced by the applied magnetic field H is specially defined as magnetostrictive strain denoted as $\lambda(\sigma, M, T)$, which is dependent on the magnetization M in Eq. (15). And it can be expressed as follows:

$$\lambda(\sigma, M, T) = -\frac{\tilde{B}}{M_s^2}(T - T_r)M^2 + \begin{cases} \frac{[1 - \tanh(\frac{\sigma}{\sigma_s})]\lambda_s}{M_s^2}M^2 & (\frac{\sigma}{\sigma_s} \geq 0) \\ \frac{[2 - \tanh(\frac{2\sigma}{\sigma_s})]\lambda_s}{2M_s^2}M^2 & (\frac{\sigma}{\sigma_s} < 0) \end{cases} \quad (16)$$

2.2 Magnetization model

As a prelude to constructing any energy-based magnetization models, it is necessary to at least qualitatively understand the basic physical mechanisms which produce hysteresis. The magnetization of magnetostrictive materials in response to applied magnetic fields is primarily due to two related mechanisms: movement of domain wall and rotation of magnetic moments [Jiles and Atherton (1986); Smith, Seelecke, Dapino, and Ounaies (2006)]. For a material that is defect free, the above mechanisms produce an anhysteretic (hysteresis-free) magnetization M_{an} that is conservative and completely reversible. Such magnetization curves are rarely observed in actual materials, however, due to the presence of defects or second-phase materials (e.g., Dysprosium in Terfenol-D) which provide minimum energy states that impede domain wall movement and subsequent rotation of magnetic moments. At low magnetic field levels, the magnetization is reversible, denoted as M_{rev} , since the domain walls remain pinned. As the field is increased, the domain walls attain sufficient energy to break the pinning sites and intersect with remote pinning sites where the energy configuration is favorable. This leads to an irreversible change in magnetization, denoted as M_{irr} , and is the fundamental cause of hysteresis behavior in magnetostrictive materials [Dapino, Smith, Faidley, and Flatau (2000)].

To quantify the anhysteretic magnetization M_{an} and the total magnetization M composed of the reversible magnetization M_{rev} and the irreversible magnetization M_{irr} , it is necessary to first determine the effective field H_{eff} which acts upon magnetic moments in the Terfenol-D rod.

Effective magnetic field

For the thermodynamics system which the present work is concerned with, the Helmholtz free energy density function $A(\sigma, M, T)$, which is the basis to quantify the effective field H_{eff} in the subsequent development, can be generally expressed

as follows [Jiles (1995)]:

$$A(\sigma, M, T) = \mu_0 H M + \frac{\mu_0}{2} \eta M^2 + \frac{3}{2} \sigma \lambda + T S \quad (17)$$

in which the dimensionless parameter η is the Weiss molecular field coefficient, which is used to quantify the amount of interaction between neighbouring magnetic moments. As mentioned above, the effective magnetic field H_{eff} causes a change in magnetization. Therefore, it can be determined by the derivative of the Helmholtz free energy density function $A(\sigma, M, T)$ with respect to magnetization M , i.e.:

$$\begin{aligned} H_{eff}(\sigma, M, T) &= \frac{1}{\mu_0} \frac{dA(\sigma, M, T)}{dM} \\ &= H + \eta M + \frac{3}{2} \frac{\sigma}{\mu_0} \frac{d\lambda}{dM} \end{aligned} \quad (18)$$

Here, the derivative of entropy density S with respect to magnetization M in magnetostrictive materials is negligible in the cases under consideration because the fields applied here do not increase the ordering within the domain, although they do lead to a change in the magnetization M .

Substituting Eq. (16) into Eq. (18) yields the final expression of the effective magnetic field H_{eff}

$$\begin{aligned} H_{eff}(\sigma, M, T) &= H + \eta M - \frac{3\tilde{B}\sigma M(T - T_r)}{\mu_0 M_s^2} \\ &+ \begin{cases} \frac{3[1 - \tanh(\frac{\sigma}{\sigma_s})]\lambda_s}{\mu_0 M_s^2} \sigma M & \left(\frac{\sigma}{\sigma_s} \geq 0\right) \\ \frac{3[2 - \tanh(\frac{2\sigma}{\sigma_s})]\lambda_s}{2\mu_0 M_s^2} \sigma M & \left(\frac{\sigma}{\sigma_s} < 0\right) \end{cases} \end{aligned} \quad (19)$$

From Eq. (19), one can find that besides the applied magnetic field and Weiss molecular field, the effective magnetic field H_{eff} includes the contribution of field relate to magnetic-elastic interactions as well as the contribution of field relate to magnetic-elastic-thermal interactions. Thus, the effective magnetic field H_{eff} derived from the Helmholtz free energy density function $A(\sigma, M, T)$ sufficiently reflects the dependences of the effective magnetic field H_{eff} on stress σ and temperature T . Here, it is worth emphasizing that the temperature dependence of the effective magnetic field which is ignored in previous studies, to our knowledge, is firstly taken into account in our theoretical model. And the final expression of the effective magnetic field H_{eff} can be expressed in a compact form

$$H_{eff}(\sigma, M, T) = H + \bar{\eta} M \quad (20)$$

where

$$\bar{\eta} = \eta - \frac{3\tilde{B}\sigma(T - T_r)}{\mu_0 M_s^2} + \begin{cases} \frac{3[1 - \tanh(\frac{\sigma}{\sigma_s})]\lambda_s \sigma}{\mu_0 M_s^2} & \left(\frac{\sigma}{\sigma_s} \geq 0\right) \\ \frac{3[2 - \tanh(\frac{2\sigma}{\sigma_s})]\lambda_s \sigma}{2\mu_0 M_s^2} & \left(\frac{\sigma}{\sigma_s} < 0\right) \end{cases} \quad (21)$$

Differentiating Eq. (20) with respect to applied magnetic field H gives

$$\frac{dH_{eff}}{dH} = 1 + \bar{\eta} \frac{dM}{dH} \quad (22)$$

Anhyseretic magnetization

For a given effective magnetic field H_{eff} , Boltzmann statistics are used to quantify the anhyseretic magnetization M_{an} in term of the Langevin function

$$M_{an} = M_s(T) \left[\coth(\kappa H_{eff}) - \frac{1}{\kappa H_{eff}} \right] \quad (23)$$

Here, $\kappa = \frac{3\chi_m}{M_s(T)}$ is the relaxation factor, χ_m stands for the magnetic susceptibility in the initial linear region. According to the theory of ferromagnetic materials [Callen (1965)], one knows that the saturation magnetization $M_s(T)$ depends on the temperature in the form

$$M_s(T) = D \left(1 - \frac{T}{T_c} \right)^x \quad (24)$$

where the exponent x and coefficient D are constants, and T_c stands for the Curie temperature of ferromagnetic materials.

When $T = T_r$, the Eq. (24) can be expressed as follows:

$$M_s = M_s(T_r) = D \left(1 - \frac{T_r}{T_c} \right)^x \quad (25)$$

The combination of Eqs. (24) and (25) yields

$$M_s(T) = M_s \frac{(T_c - T)^x}{(T_c - T_r)^x} \quad (26)$$

in which $x = \frac{1}{2}$ for the Weiss molecular field theory and $T_c = 383.3^\circ\text{C}$ for Terfenol-D [Dhilsha and Rama Rao (1993)].

Substituting Eq. (26) into Eq. (23) yields the final expression of the anhysteretic magnetization M_{an}

$$M_{an} = M_s \frac{(T_c - T)^x}{(T_c - T_r)^x} \times \left[\coth \left(\frac{3\chi_m (T_c - T_r)^x}{M_s (T_c - T)^x} H_{eff} \right) - \frac{M_s (T_c - T)^x}{3\chi_m (T_c - T_r)^x H_{eff}} \right] \quad (27)$$

Differentiating Eq. (27) with respect to efficient magnetic field H_{eff} gives

$$\frac{dM_{an}}{dH_{eff}} = \frac{M_s^2 (T_c - T)^{2x}}{3\chi_m (T_c - T_r)^{2x} H_{eff}^2} - \frac{3\chi_m}{\sinh^2 \left(\frac{3\chi_m (T_c - T_r)^x}{M_s (T_c - T)^x} H_{eff} \right)} \quad (28)$$

Total magnetization composed of reversible and irreversible magnetization

As indicated previous and elsewhere [Calkins, Smith, and Flatau (2000)], the anhysteretic magnetization M_{an} can only be used to model the magnetization for ideal or perfect magnetostrictive materials. As a kind of typical magnetostrictive materials, however, Terfenol-D rods have defects or second-phase materials which impede the change in magnetization. The present work is not concerned with the nature of these defects and they will be referred to collectively as pinning sites. These pinning sites are the fundamental causes of hysteresis behavior and energy loss in the magnetization progress. The energy loss δL_{mag} per unit volume to these pinning sites is modeled assuming a friction-type mechanism which opposes changes in magnetization, and expressed as a function of the irreversible magnetization M_{irr} [Jiles and Atherton (1986)] by the equation

$$\delta L_{mag} = \mu_0 \int \zeta K (1 - c) dM_{irr} \quad (29)$$

where the non-negative constant K is a micro-structural parameter with dimensions of magnetic field, which is proportional to the pinning sites density and pinning sites energy, and provides a measure for the average energy required to break a pinning site. The dimensionless parameter c is a reversibility coefficient and can be estimated from the ratio of the initial and anhysteretic differential susceptibilities. The parameter ζ takes the value $+1$ when the applied magnetic field H increases and -1 when the applied magnetic field H decreases to ensure that the pinning sites always oppose changes in magnetization.

For this thermodynamics system, the energy balance principle can be generally expressed as

$$\delta W_{bat} = \delta W_{mag} + \delta L_{mag} \quad (30)$$

Here, δW_{bat} stands for the work done per unit volume by the applied magnetic field H , δW_{mag} stands for the change in the energy density of the materials, and they can be respectively expressed as follows [Iyer and Krishnaprasad (2005)]

$$\delta W_{bat} = -\mu_0 \int M dH_{eff} \quad (31)$$

$$\delta W_{mag} = -\mu_0 \int M_{an} dH_{eff} \quad (32)$$

Substituting Eqs. (29), (31) and (32) into Eq. (30) yields

$$-\mu_0 \int M dH_{eff} = -\mu_0 \int M_{an} dH_{eff} + \mu_0 \int \zeta K (1 - c) dM_{irr} \quad (33)$$

Differentiating Eq. (33) with respect to the effective magnetic field H_{eff} , and then dividing by μ_0 gives

$$\frac{dM_{irr}}{dH_{eff}} = \frac{M_{an} - M}{\zeta K (1 - c)} \quad (34)$$

According to the postulates of Jiles and Atherton, the following relationship [Iyer and Krishnaprasad (2005)] can be obtained

$$\frac{dM}{dH} = \delta_M (1 - c) \frac{dM_{irr}}{dH} + c \frac{dM_{an}}{dH} \quad (35)$$

in which

$$\delta_M = \begin{cases} 0: & \dot{H} < 0 \text{ and } M_{an} - M > 0, \\ 0: & \dot{H} > 0 \text{ and } M_{an} - M < 0, \\ 1: & \text{otherwise.} \end{cases} \quad (36)$$

Here, the parameter δ_M is used to guarantee that the calculation results are coincident with the physical properties of Terfenol-D. Without this parameter, the incremental susceptibility at the reversal points $\frac{dM}{dH}$ will become negative, which is a nonphysical behavior for Terfenol-D. This can be checked by numerical simulations.

Multiplying both sides of Eq. (35) by $\frac{dH}{dH_{eff}}$, and applying the chain rule, Eq. (35) can be modified as follows:

$$\frac{dM}{dH_{eff}} = \delta_M (1 - c) \frac{dM_{irr}}{dH_{eff}} + c \frac{dM_{an}}{dH_{eff}} \quad (37)$$

Substituting Eqs. (28) and (34) into (37) yields

$$\frac{dM}{dH_{eff}} = \frac{\delta_M (M_{an} - M)}{\zeta K} + \frac{cM_s^2 (T_c - T)^{2x}}{3\chi_m (T_c - T_r)^{2x} H_{eff}^2} - \frac{3c\chi_m}{\sinh^2 \left(\frac{3\chi_m (T_c - T_r)^x}{M_s (T_c - T)^x} H_{eff} \right)} \quad (38)$$

Multiplying both sides of Eq. (38) by $\frac{dH_{eff}}{dH}$, and applying the chain rule, Eq. (38) can be rewritten as follows:

$$\frac{dM}{dH} = \left[\frac{\delta_M (M_{an} - M)}{\zeta K} + \frac{cM_s^2 (T_c - T)^{2x}}{3\chi_m (T_c - T_r)^{2x} H_{eff}^2} - \frac{3c\chi_m}{\sinh^2 \left(\frac{3\chi_m (T_c - T_r)^x}{M_s (T_c - T)^x} H_{eff} \right)} \right] \frac{dH_{eff}}{dH} \quad (39)$$

Substituting Eq. (22) into Eq. (39) and after some mathematical manipulations, the differential equation of the magnetization model (i.e., the differential susceptibility of the total magnetization M) can be obtained as follows

$$\begin{aligned} \frac{dM}{dH} = & \left\{ \left[3\delta_M \chi_m (T_c - T_r)^{2x} H_{eff}^2 (M_{an} - M) + \zeta K c M_s^2 (T_c - T)^{2x} \right] \right. \\ & \times \left. \sinh^2 \left(\frac{3\chi_m (T_c - T_r)^x}{M_s (T_c - T)^x} H_{eff} \right) - 9\zeta K c \chi_m^2 (T_c - T_r)^{2x} H_{eff}^2 \right\} \\ & \div \left\{ \left[3\chi_m (T_c - T_r)^{2x} H_{eff}^2 (\zeta K - \delta_M \bar{\eta} M_{an} + \delta_M \bar{\eta} M) \right. \right. \\ & \left. \left. - \bar{\eta} \zeta K c M_s^2 (T_c - T)^{2x} \right] \times \sinh^2 \left(\frac{3\chi_m (T_c - T_r)^x}{M_s (T_c - T)^x} H_{eff} \right) \right. \\ & \left. + 9\bar{\eta} \zeta K c \chi_m^2 (T_c - T_r)^{2x} H_{eff}^2 \right\} \quad (40) \end{aligned}$$

which after numerical integration gives the total magnetization M from the application of a magnetic field H .

The magnetization model (40) and the magnetostriction model (15) can be combined to constitute a general coupled magnetic-elastic-thermal free-energy model with hysteretic nonlinearity for Terfenol-D rods, in which the variables H_{eff} and M_{an} are given by Eqs. (19) and (27), respectively. From the viewpoint of numerical solutions for this free-energy model, it is most convenient to first solve Eq. (40) via Adams-type predictor-corrector method for the total magnetization M , and then

the magnetostrictive strain λ under a variety of conditions of mechanical stress and applied field as well as working temperature can be obtained from Eq. (16). The magnetic flux density B in Terfenol-D rods can be determined by

$$B = \mu_0 (M + H) \quad (41)$$

At the end of this section, it should be noted that the free-energy model established here does not incorporate the eddy-current losses so, to avoid simulation inaccuracies, it should be employed in low frequency drive regimes. The inclusion of eddy-current losses can be addressed by adding appropriate terms in the energy relations, and the extension of this model to incorporate eddy-current losses is under current investigation. In this article, we mainly investigate the symmetric major loops of Terfenol-D under quasi-static operating conditions. However, the free-energy model established in this article can also be extended to accurately predict minor loops of Terfenol-D, which will be discussed in another article in details. For the operating conditions targeted in this article, the validity and reliability of the free-energy model are illustrated in the next section.

3 Experimental verification and discussion

In order to verify the validity and reliability of the free-energy model established in Sec. 2, in this section, comparisons between its predictions and Slaughter *et al.* [Slaughter, Dapino, Smith, and Flatau (2000)] experimental data are firstly given. After that, the effect of the Weiss molecular field, and the influences of the mechanical stress and the temperature on the magnetostrictive effect of Terfenol-D are discussed in detail by using this free-energy model.

3.1 Experimental verification

To comply with the experimental conditions [Slaughter, Dapino, Smith, and Flatau (2000)], the compressive stress and temperature are respectively taken as 1500psi and 18°C, and the amplitude of applied magnetic field is taken as 110kA / m. The parameters appeared in the free-energy model are respectively chosen as $M_s = 7.65 \times 10^5 \text{ A / m}$, $\lambda_s = 1950 \times 10^{-6}$, $\sigma_s = 200 \times 10^6 \text{ Pa}$, $\tilde{B} = 2.5 \times 10^{-6} \text{ }^\circ\text{C}^{-1}$, $\chi_m = 20.4$, $K = 6000 \text{ A / m}$, $c = 0.1$ and $\eta = 0.082$, which are also in accordance with the parameters given in the reference [Slaughter, Dapino, Smith, and Flatau (2000)] and are used in succeeding numerical simulations. The comparisons of relative magnetization hysteresis loop and magnetostrictive strain hysteresis loop for Terfenol-D between the numerical simulation results predicted by the free-energy model established in this article and Slaughter *et al.* [Slaughter, Dapino, Smith, and Flatau (2000)] experimental data are, respectively, shown in Figs. 1(a) and 1(b). As is

evident in these two figures, the calculated results are perfectly coincident with the experimental data not only in quality but also in quantity. It indicates that the free-energy model established in this article can accurately capture nonlinear hysteresis characteristics for Terfenol-D not only in the region of the low and moderate magnetic fields but also in the region of the high magnetic field, especially for the nonlinear hysteresis and saturation present in the region of the high magnetic field.

3.2 The effect of Weiss molecular field

According to Weiss molecular field theory, there is strong interaction between neighboring magnetic moments of Terfenol-D, and it is modeled by Weiss molecular field. In order to reflect the effect of Weiss molecular field, here, we ignore Weiss molecular field effect (i.e., taking $\eta = 0$) and compare its predictions with Slaughter *et al.* [Slaughter, Dapino, Smith, and Flatau (2000)] experimental data in Figs. 2(a) and 2(b), in which the original predictions with Weiss molecular field effect (i.e., taking $\eta = 0.082$) are also illustrated for reference. From the comparisons, it can be found that the theoretical predictions without Weiss molecular field effect markedly underestimate the experimental data of both relative magnetization hysteresis loop and magnetostrictive strain hysteresis loop for Terfenol-D, especially for magnetostrictive strain hysteresis loop. These large discrepancies indicate the necessity of incorporating Weiss molecular field into the effective magnetic field H_{eff} and support the conclusion of Weiss molecular field theory.

3.3 The influence of the compressive stress

Mechanical stress is considered one of the primary factors, along with magnetic field and temperature, which influences the magnetostrictive effect of Terfenol-D [Tremolet and Etienne (1993)]. Therefore, it is of particular importance to thoroughly investigate the influence of stress on the magnetostrictive effect of Terfenol-D. Because Terfenol-D is often operated in compressive stress conditions, here, the free-energy model established in this article is used to investigate the influence of compressive stress on the magnetostrictive effect of Terfenol-D in detail. However, the present free-energy model can also be used to investigate the influence of tensile stress as mentioned above. Figs. 3(a) and 3(b) give out the hysteresis loops of relative magnetization $\frac{M}{M_s}$ versus applied magnetic field H and magnetostrictive strain λ versus applied magnetic field H under different compressive stress from 1.5 ksi to 6.0 ksi (as the arrow indicates) with fixed temperature of $T = 18^\circ\text{C}$, respectively. From Fig. 3(a), it can be found that the values of the relative magnetization $\frac{M}{M_s}$ increase with the applied magnetic field H under different compressive stress, and will reach a same constant in the region of the high field,

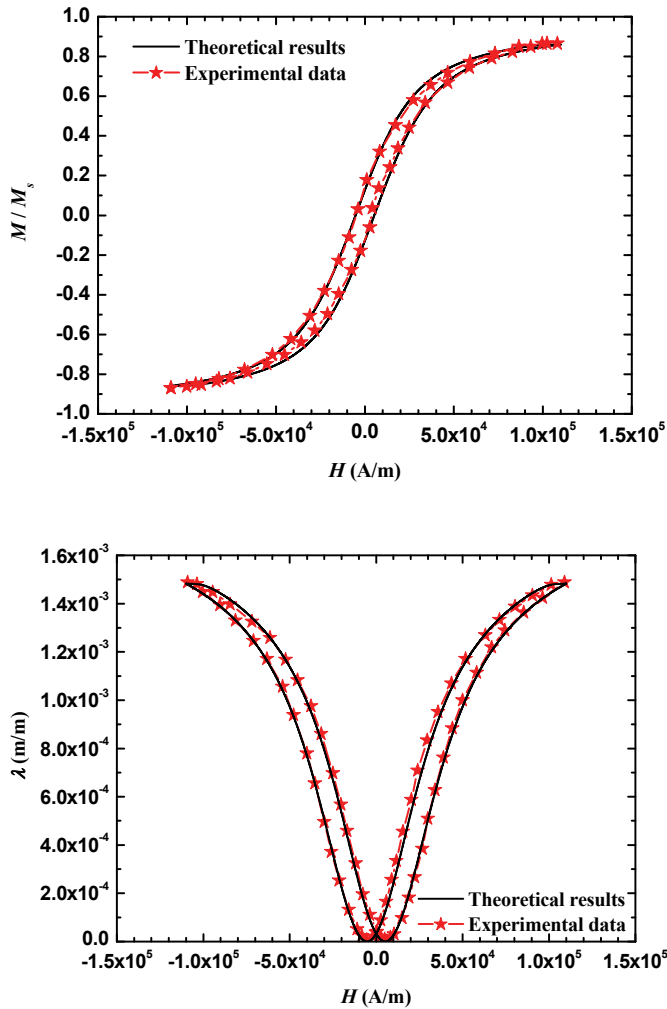


Figure 1: (a) Comparison of relative magnetization hysteresis loop between experimental measurements and theoretical predictions. (b) Comparison of magnetostrictive strain hysteresis loop between experimental measurements and theoretical predictions.

which means that the maximum magnetization is independent on the compressive stress. At the same time, the slopes of the relative magnetization hysteresis loops decrease with an increasing compressive stress in the region of the low and moderate magnetic fields, which implies that the relative magnetization $\frac{M}{M_s}$ induced by

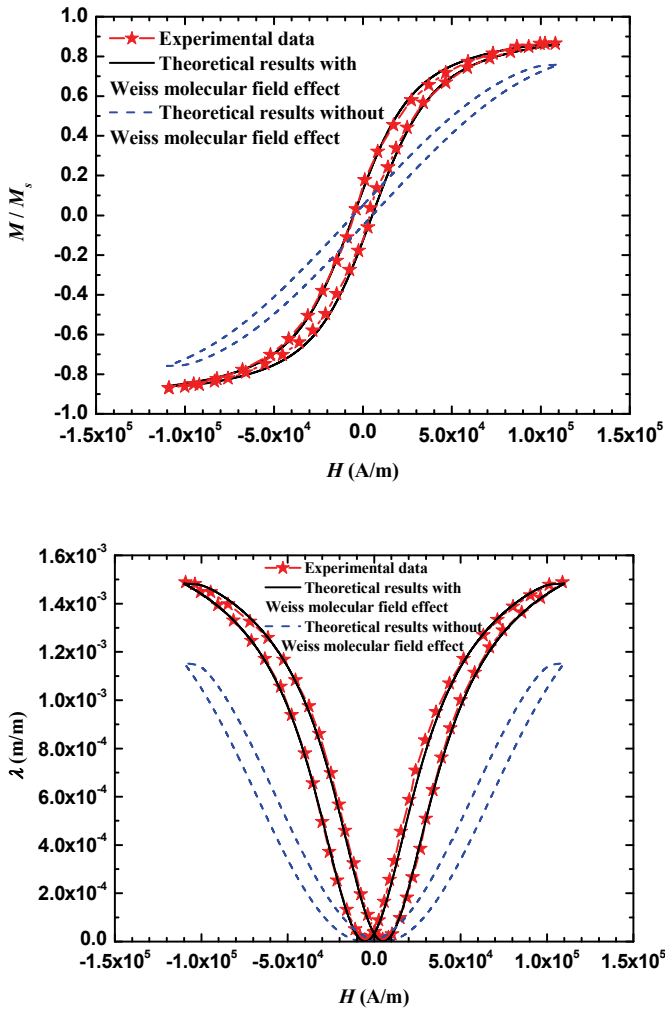


Figure 2: (a) Comparison of relative magnetization hysteresis loop between experimental measurements and theoretical predictions without Weiss molecular field effect. The theoretical predictions with Weiss molecular field effect are illustrated for reference. (b) Comparison of magnetostrictive strain hysteresis loop between experimental measurements and theoretical predictions without Weiss molecular field effect. The theoretical predictions with Weiss molecular field effect are illustrated for reference.

per unit applied magnetic field H gradually decreases as the compressive stress increases. For Terfenol-D, an explanation for this phenomenon could be that when the compressive stress is high the domain movement requires more magnetic energy, and therefore the material is unable to respond to the applied magnetic field H as well as it can when the compressive stress is lower. Both the values of magnetostrictive strain and the slopes of magnetostrictive strain hysteresis loops shown in Fig. 3(b) decrease with an increasing compressive stress in the region of the low and moderate magnetic fields. It is similar to the relative magnetization hysteresis loops shown in Fig. 3(a). However, the similarity only takes place in the region of the low and moderate fields. When the applied magnetic field H is in the high field region, the magnetostrictive strain of Terfenol-D will reach the different maximum values from 1830×10^{-6} at -1.5ksi to 2040×10^{-6} at -6.0ksidue to the fact that more magnetic domains are aligned perpendicular to the external force to keep the minimum energy state when a higher compressive stress is applied on the Terfenol-D. It is the well-known “overturn phenomenon” observed in the experiments [Butler (1988); Clark, Teter, and McMasters (1988); Liang and Zheng (2007); Moffett, Clark, Wun-Fogle, Linberg, Teter, and McLaughlin (1991)], which can not be predicted by the previous physics-based hysteresis model. The detailed information about the maximum magnetostrictive strain is listed in Tab. 1. All of above results predicted by the free-energy model established in this article are consistent with the observed experimental phenomena [Butler (1988); Clark, Teter, and McMasters (1988); Liang and Zheng (2007); Moffett, Clark, Wun-Fogle, Linberg, Teter, and McLaughlin (1991)], especially for “overturn phenomenon”, which confirms that the present free-energy model can adequately capture the nonlinear magnetic-elastic coupling characteristic with hysteresis for Terfenol-D.

As noted in previous discussion, the compressive stress has obvious influence on the slopes of magnetization hysteresis loops and magnetostrictive strain hysteresis loops. In order to quantify this kind of influence in detail, the susceptibility (i.e., the derivative of magnetization M with respect to the applied magnetic field H) and the piezomagnetic coefficient (Note that the derivative of magnetostrictive strain λ with respect to the applied magnetic field H is named the piezomagnetic coefficient

Table 1: Physical parameters for Terfenol-D rods

$\sigma(\text{ksi})$	$\left(\frac{dM}{dH}\right)_{\max}$	$\lambda_{\max}(10^{-6})$	$A_{\text{loss}}(\text{A} / \text{m})$	$\left(\frac{d\lambda}{dH}\right)_{\max}(10^{-9}\text{A}^{-1} \cdot \text{m})$	$H_{\max}(\text{kA} / \text{m})$
-1.5	18.66639	1830	39.71496	29.46469	15.86
-3.0	6.74907	1910	41.67342	15.17966	63.44
-4.5	4.04562	1980	43.19914	10.78696	116.86
-6.0	2.81783	2040	44.43571	8.46397	177.12

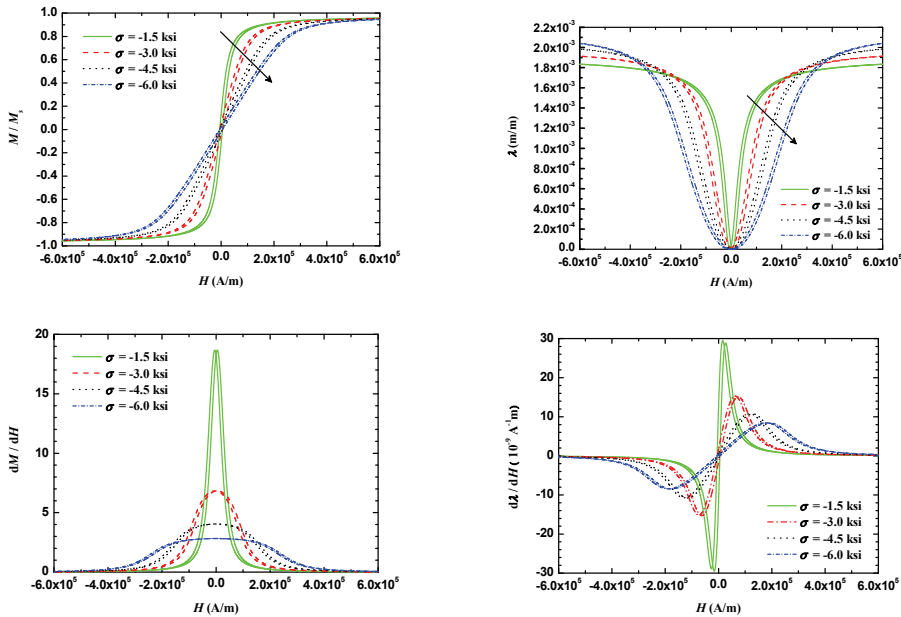


Figure 3: (a) Hysteresis loops of relative magnetization versus applied magnetic field under different compressive stress from 1.5 ksi to 6.0 ksi with fixed temperature of $T = 18^\circ\text{C}$. (b) Hysteresis loops of magnetostrictive strain versus applied magnetic field under different compressive stress from 1.5 ksi to 6.0 ksi with fixed temperature of $T = 18^\circ\text{C}$. (c) Hysteresis loops of susceptibility versus applied magnetic field under different compressive stress from 1.5 ksi to 6.0 ksi with fixed temperature of $T = 18^\circ\text{C}$. (d) Hysteresis loops of piezomagnetic coefficient versus applied magnetic field under different compressive stress from 1.5 ksi to 6.0 ksi with fixed temperature of $T = 18^\circ\text{C}$.

in order to be consistent with the nomenclature adopted in the reference [Moffett, Clark, Wun-Fogle, Linberg, Teter, and McLaughlin (1991)], despite that there is not true piezomagnetism in the Terfenol-D discussed in this article.) as functions of the applied magnetic field H under different compressive stress from 1.5 ksi to 6.0 ksi with fixed temperature of $T = 18^\circ\text{C}$ are respectively plotted in Figs. 3(c) and 3(d), which are obtained by differential calculations for Figs. 3(a) and 3(b), respectively. As is evident in these two figures, the susceptibility $\frac{dM}{dH}$ has an even symmetry with respect to the applied magnetic field H , while the piezomagnetic coefficient $\frac{d\lambda}{dH}$ is of odd symmetry with respect to the applied magnetic field H . Meanwhile, both the susceptibility $\frac{dM}{dH}$ and the piezomagnetic coefficient $\frac{d\lambda}{dH}$ are not constants, and

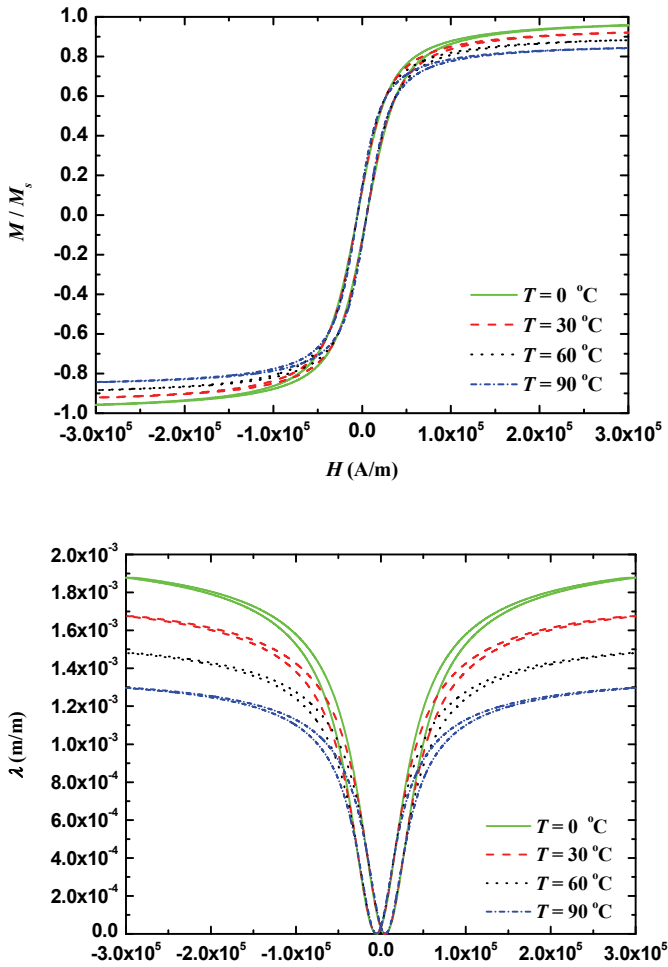


Figure 4: (a) Hysteresis loops of relative magnetization versus applied magnetic field under different temperature from 0°C to 90°C with fixed compressive stress of $\sigma = -1.5\text{ksi}$. (b) Hysteresis loops of magnetostrictive strain versus applied magnetic field under different temperature from 0°C to 90°C with fixed compressive stress of $\sigma = -1.5\text{ksi}$.

dependent on the compressive stress, the applied magnetic field and the magnetization history. The maximum susceptibility (denoted as $\left(\frac{dM}{dH}\right)_{\max}$) is obtained near zero magnetic field. Both the maximum susceptibility and the maximum piezomagnetic coefficient (denoted as $\left(\frac{d\lambda}{dH}\right)_{\max}$) decrease with an increasing compressive stress, especially for the maximum susceptibility, while the applied magnetic fields (denoted as H_{\max}) associated with the maximum piezomagnetic coefficient increase from 15.86kA / m to 177.12kA / m with an increasing compressive stress, which is in agreement with the experimental measurement and theoretical prediction without considering hysteresis of single-crystal iron-gallium alloys in quality [Atulasima, Flatau, and Cullen (2008)]. However, the range of applied magnetic field H , in which the higher susceptibility and piezomagnetic coefficient are obtained, enlarges with an increasing compressive stress. The detailed information about the maximum susceptibility and the maximum piezomagnetic coefficient as well as the corresponding applied magnetic field is summarized in Tab. 1. Except the information mentioned previous, Tab. 1 also shows the areas of the magnetostrictive strain hysteresis loops under different compressive stress (denoted as A_{loss}), all of which are important parameters considered in practical application. Finally, it is worth noting that these laws described by the free-energy model established in this article are coincident with the experimental results of Terfenol-D in qualitatively [Gao, Pei, and Fang (2008); Moffett, Clark, Wun-Fogle, Linberg, Teter, and McLaughlin (1991)].

3.4 The influence of the temperature

Discussing the influence of the temperature by the free-energy model established in this article comprises the final component of this investigation. Figs. 4(a) and 4(b) show the hysteresis loops of relative magnetization $\frac{M}{M_s}$ versus applied magnetic field H and magnetostrictive strain λ versus applied field H under different temperature from 0°C to 90°C with fixed compressive stress of $\sigma = -1.5\text{ksi}$, respectively. As shown in these two figures, the temperature does not have remarkable influence on the slopes of the relative magnetization hysteresis loops and the magnetostrictive strain hysteresis loops in the region of the low and moderate magnetic fields. When the applied magnetic field H is in the high field region, however, both the relative magnetization $\frac{dM}{dH}$ and the magnetostrictive strain λ of Terfenol-D decrease fairly linearly with an increasing temperature, just like the results shown in experiment [Clark, and Crowder (1985); Clark, Teter, and McMasters (1988)]. It indicates that the free-energy model established in this article can efficiently capture the influence of the temperature on the magnetostrictive effect of Terfenol-D.

4 Conclusions

In this article, a novel free-energy model simultaneously incorporating nonlinear hysteresis and magnetic-elastic-thermal coupling constitutive behavior inherent to Terfenol-D is established on the basis of the thermodynamic theory and the postulates of Jiles and Atherton, in which the effect of Weiss molecular field is incorporated. After that, the validity and reliability of the obtained free-energy model are verified by comparing its predicted results with existing experimental data, and the comparison results also indicate that the free-energy model can accurately capture the nonlinear hysteresis characteristic of Terfenol-D not only in the region of the low and moderate magnetic fields but also in the region of the high magnetic field. Meanwhile, the influences of mechanical stress and the temperature on the magnetostrictive effect of Terfenol-D are thoroughly investigated by using this free-energy model. The numerical simulation results are consistent with some well-known experimental results in quality or in quantity, such as the temperature-dependent saturation nonlinearity and “overturn phenomenon”, which indicates that the free-energy model can also effectively capture the nonlinear magnetic-elastic-thermal coupling characteristic of Terfenol-D. Moreover, some important physical parameters, such as the maximum magnetostrictive strain, the maximum piezomagnetic coefficient, are predicted by the proposed free-energy model, which can be used to optimize the performance of Terfenol-D in practical application. Finally, it should be noted that there are only a small number of parameters appeared in the free-energy model. All of them have definite physical implications, and can be easily determined by experiments. Therefore, the free-energy model established in this article provides the capability for simultaneously and conveniently capturing nonlinear hysteresis and magnetic-elastic-thermal coupling constitutive behavior inherent to Terfenol-D, and can be conveniently used in the practical engineering application.

Acknowledgement: This research was supported by Grant No. 10972094 of the Fund of Natural Science Foundation of China, the Fund of Ministry of Education of the Program of Changjiang Scholars and Innovative Research Team in University (No. IRT0628), and the Science Foundation of the Ministry of Education of China for the Ph.D. program. The authors gratefully acknowledge these supports.

References

AI-Jiboory, M.; Lord, D. G. (1990): Study of the magnetostrictive distortion in single crystal Terfenol-D by X-ray diffraction. *IEEE Transactions on Magnetics*, vol. 26, no. 5, pp. 2583-2585.

Atulasima, J.; Flatau, A. B.; Cullen, J. R. (2008): Energy-based quasi-static modeling of the actuation and sensing behavior of single-crystal iron-gallium alloys. *Journal of Applied Physics*, vol. 103, pp. 014901.

Bergqvist, A.; Engdahl, G. (1991): A stress-dependent magnetic Preisach hysteresis model. *IEEE Transactions on Magnetics*, vol. 27, no. 6, pp. 4796-4798.

Butler, J. L. (1988): *Application Manual for Design of Etrema Terfenol-D Magnetostrictive Transducers*. Edge Technologies.

Calkins, F. T.; Smith, R. C.; Flatau, A. B. (2000): Energy-based hysteresis model for magnetostrictive transducers. *IEEE Transactions on Magnetics*, vol. 36, no. 2, pp. 429-439.

Callen, E. (1965): Ferromagnetic transitions and the one-third-power law. *Journal of Applied Physics*, vol. 36, pp. 1140-1142.

Carman, G. P.; Mitrovic, M. (1995): Nonlinear constitutive relations for magnetostrictive materials with applications to 1-D problems. *Journal of Intelligent Material Systems and Structures*, vol. 6, pp. 673-683.

Clark, A. E. (1980): *in Ferromagnetic Materials*. North-Holland Press.

Clark, A. E.; Crowder, D. N. (1985): High temperature magnetostriction of TbFe_2 and $\text{Tb}_{0.27}\text{Dy}_{0.73}\text{Fe}_2$. *IEEE Transactions on Magnetics*, vol. 21, no. 5, pp. 1945-1947.

Clark, A. E.; Teter, J. P.; McMasters, O. D. (1988): Magnetostriction “jumps” in twinned $\text{Tb}_{0.3}\text{Dy}_{0.7}\text{Fe}_{1.9}$. *Journal of Applied Physics*, vol. 63, no. 8, pp. 3910-3912.

Dhilsha, K. R.; Rama Rao, K. V. S. (1993): Investigation of magnetic magnetomechanical, and electrical properties of the $\text{Tb}_{0.27}\text{Dy}_{0.73}\text{Fe}_{2-x}\text{Co}_x$ system. *Journal of Applied Physics*, vol. 73, no. 3, pp. 1380-1385.

Duenas, T. A.; Hsu, L.; Carman, G. P. (1996): Magnetostrictive composite material systems analytical/experimental (Invited article). *in Advances in Materials for Smart Systems-Fundamental and Applications*, pp. 527-543.

Gao, X.; Pei, Y. M.; Fang, D. N. (2008): Magnetomechanical behaviors of giant magnetostrictive materials. *Acta Mechanica Solida Sinica*, vol. 21, no. 1, pp. 15-18.

Iyer, R. V.; Krishnaprasad, P. S. (2005): On a low-dimensional model for ferromagnetism. *Nonlinear Analysis*, vol. 61, pp. 1447-1482.

Jiles, D. C.; Atherton, D. L. (1983): Ferromagnetic hysteresis. *IEEE Transactions on Magnetics*, vol. 19, no. 5, pp. 2183-2185.

Jiles, D. C.; Atherton, D. L. (1986): Theory of ferromagnetic hysteresis. *Journal*

of Magnetism and Magnetic Materials, vol. 61, pp. 48-60.

Jiles, D. C.; Hariharan, S. (1990): Interpretation of the magnetization mechanism in Terfenol-D using Barkhausen pulse-height analysis and irreversible magnetostriction. *Journal of Applied Physics*, vol. 67, no. 9, pp. 5013-5015.

Kellogg, R.; Flatau, A. (1999): Blocked force investigation of a Terfenol-D transducer. *SPIE's 6th Annual International Symposium on Smart Structures and Materials*, vol. 3668, pp. 184-195.

Liang, Y. R.; Zheng, X. J. (2007): Experimental researches on magneto-thermo-mechanical characterization of Terfenol-D. *Acta Mechanica Solida Sinica*, vol. 20, no. 4, pp. 283-288.

Liu, X. E.; Zheng, X. J. (2005): A nonlinear constitutive model for magnetostrictive materials. *Acta Mechanica Sinica*, Vol. 21, pp. 278-285.

Moffett, M. B.; Clark, A. E.; Wun-Fogle, M.; Linberg, J.; Teter, J. P.; McLaughlin, E. A. (1991): Characterization of Terfenol-D for magnetostrictive transducers. *Journal of the Acoustical Society of America*, vol. 89, no. 3, pp. 1448-1455.

Olabi, A. G.; Grunwald, A. (2008): Design and application of magnetostrictive materials. *Materials & Design*, vol. 29, pp. 469-483.

Slaughter, J. C.; Dapino, M. J.; Smith, R. C.; Flatau, A. B. (2000): Modeling of a Terfenol-D ultrasonic transducer. *Proceedings of SPIE Symposium on Smart Structures and Materials*, vol. 3985, pp. 366-377.

Smith, R. C.; Seelecke, S.; Dapino, M.; Ounaies, Z. (2006): A unified framework for modeling hysteresis in ferroic materials. *Journal of the Mechanics and Physics of Solids*, vol. 54, pp. 46-85.

Wan, Y. P.; Fang, D. N.; Hwang, K. C. (2003): Non-linear constitutive relations for magnetostrictive materials. *International Journal of Non-Linear Mechanics*, vol. 38, pp. 1053-1065.

Wang, T. Z.; Zhou, Y. H. (2010): A theoretical study of nonlinear magnetoelectric effect in magnetostrictive-piezoelectric trilayer. *Composite Structures*, vol. 93, pp. 1485-1492.

Wang, Z. C. (1992): *Thermodynamics and Statistical Physics*. Higher Education Press (in Chinese).

Zheng, X. J.; Liu, X. E. (2005): A nonlinear constitutive model for Terfenol-D rods. *Journal of Applied Physics*, vol. 97, pp. 053901.

Zhou, H. M.; Li, F.; Ye, Q.; Zhao, J. X.; Xia, Z. L.; Tang, Y.; Wei, J. (2010): Young's modulus measurement of thin films by resonant frequency method using magnetostrictive resonator. *CMC: Computers, Materials, & Continua*, vol. 13, no. 3, pp. 235-248.

Zhou, H. M.; Zhou, Y. H.; Zheng, X. J. (2007): Numerical simulation of nonlinear dynamic responses of beams laminated with giant magnetostrictive actuators. *CMC: Computers, Materials, & Continua*, vol. 6, no. 3, pp. 201-211.

Zhou, H. M.; Zhou, Y. H.; Zheng, X. J.; Wei, J. (2009): A general magnetoelastic coupling theory of deformable magnetized medium including magnetic forces and magnetostriction effects. *CMC: Computers, Materials, & Continua*, vol. 12, no. 3, pp. 237-249.